Materials and Design 80 (2015) 1–11

Contents lists available at ScienceDirect

Materials and Design

journal homepage: www.elsevier.com/locate/matdes

Ni–W/ZrO_2 nanocomposites obtained by ultrasonic DC electrodeposition

E. Beltowska-Lehman [a,*], P. Indyka [b], A. Bigos [a], M.J. Szczerba [a], M. Kot [c]

[a] Institute of Metallurgy and Materials Science of the Polish Academy of Sciences, 25 Reymonta St., 30-059 Krakow, Poland
[b] Faculty of Chemistry, Jagiellonian University, 3 Ingardena St., 30-060 Krakow, Poland
[c] Faculty of Mechanical Engineering and Robotics, AGH University of Science and Technology, 30 Mickiewicza Av., 30-059 Krakow, Poland

ARTICLE INFO

Article history:
Received 9 January 2015
Revised 5 April 2015
Accepted 30 April 2015
Available online 1 May 2015

Keywords:
Metal matrix nanocomposites
Ultrasonic electrodeposition
Ni–W coatings
Ni–W/ZrO_2 composite coatings
Zirconia nanoparticles

ABSTRACT

Composite coatings consisting of a nanocrystalline Ni–W alloy matrix reinforced with ZrO_2 particles (average size of 50 nm) were synthesized by electrochemical deposition assisted by an external ultrasonic field. The Ni–W/ZrO_2 coatings were deposited from aqueous sulphate–citrate electrolytes containing zirconia nanopowder in suspension on steel substrates in a system with a rotating disk electrode (RDE). The influence of relevant processing parameters (i.e., concentration of zirconia powder in plating bath, current density, hydrodynamic conditions, ultrasonic field frequency) on the composite characteristics was discussed. Based on micromechanical (microhardness, Young's modulus) and microstructural (morphology, phase composition, crystallite size) properties of the coatings, the conditions for electrodeposition of crack-free, homogeneous Ni–W/ZrO_2 nanocomposites with enhanced functional properties have been developed.

1. Introduction

The increasing demand for advanced materials with precisely controlled properties has led to interest in the development of metal matrix composites (MMCs). These innovative materials possess almost unlimited possibilities for material engineering, as their properties can be designed depending on the application [1]. The properties of MMCs are mainly determined by the combination of components as well as by their interfacial characteristics. MMC coatings are usually designed to improve surface tribological properties, since metals are dispersion hardened by the incorporation of ceramic particles. Different types of particles with a variety of properties, e.g., oxides (Al_2O_3, ZrO_2), carbides (SiC, WC, SiC), nitrides (Si_3N_4) and borides (TiB_2, ZrB_2), have been commonly used to reinforce matrices of microcrystalline metals or alloys [2,3]. Composites with a nanocrystalline metallic matrix are characterized by significantly greater hardness and strength than their microcrystalline counterparts, due to the high grain boundary densities leading to enhanced or novel properties [4]. The selection of a matrix and ceramic dispersive phase is mainly determined by the intended use of resulting composites. The chemical composition, grain size, residual stresses and structural defects are important for the metallic matrix, whereas ceramic component is characterized by type, size, shape, amount and distribution of particles.

Metal matrix composite materials can be produced by different technologies [5]. The most widely applied methods for MMC production are powder metallurgy, casting techniques, hot pressing, oxidation, nitridation and thermal spraying. However, high temperatures, elevated pressures and expensive, complicated equipment are main disadvantages of these techniques. Electrodeposition is considered one of the most important techniques for producing nanocomposites, at a low cost and high deposition rate [6].

Electrodeposition (also termed 'electroplating' or 'electrochemical deposition') involves the deposition of metallic coatings on a conductive cathode by electrolysis of aqueous electrolyte solutions, at ambient temperature, under normal pressure. Coatings of nanosized grains can be easy achieved by controlling deposition parameters [7]. In electrochemical composite deposition, inert ceramic particles are suspended in the plating bath, and then embedded during the direct current (DC) electrodeposition of metal matrix. The incorporation of homogeneously dispersed ceramic particles into a metallic matrix leads to the development of composites with enhanced or totally new engineering properties. The electrodeposition technique enables the synthesis of a wide range of metal matrix ceramic composites by the application of various types of particles, combined with different electrolyte solutions. Hence, in recent years, a rapid increase in interest in metal matrix nanocomposites produced by electrodeposition has been observed [3]. The nickel-based alloys are widely applied as composite matrices due to their superior properties [8,9]. For example,

* Corresponding author.
E-mail address: nmbeltow@imim-pan.krakow.pl (E. Beltowska-Lehman).

http://dx.doi.org/10.1016/j.matdes.2015.04.049
0261-3069/

most metallic microcomponents are currently produced in the LIGA process, which involves selective electrodeposition of nanocrystalline Ni into lithographic molds. However, nanostructured nickel is generally unstable, which may lead to a rapid grain growth even at low temperatures [9]. Alloying with some metals of high melting points has been found to improve stability of that system [10].

Among these materials, nanocrystalline Ni–W alloys are known for excellent characteristics, such as stability, high hardness (including hot hardness), high wear resistance at elevated temperatures, high melting point, low coefficient of thermal expansion, high tensile strength and high corrosion resistance in many aggressive environments [11–13]. Recently, it was found that the incorporation of different ceramic particles (e.g., Al_2O_3, TiO_2, SiC, WC, CeO_2, etc.) into Ni–W deposits can improve the tribological and micromechanical properties of the resulting composites [14–18]. However, composite coatings of a nanostructured Ni–W matrix reinforced by zirconia (ZrO_2) nanoparticles are new materials, although the possibility of fabrication Ni–W/ZrO_2 coatings by electrochemical methods has been presented in a recently published paper [19]. Also, so far only a few publications were devoted to pure nickel coatings containing ZrO_2 particles, while zirconia (extremely refractory material) offers high hardness, high wear resistance and chemical inertness [20–22]. Indeed, it was reported that Ni/ZrO_2 nanocomposite coatings have been successfully prepared under DC electrodeposition and the embedded zirconia particles have resulted in enhancing the wear and corrosion resistance of the Ni matrix. Thus, it would be expected that the incorporation of zirconium oxide as ceramic hard particles into Ni–W alloy matrix allows composites of outstanding characteristics to be obtained, taking into account the properties of both components and their nanocrystalline microstructure. Moreover, the results of our previous study on electrodeposition and characterization of Ni/Al_2O_3 and Ni–W/Al_2O_3 composites showed a significant improvement of the microhardness and wear resistance as compared to the pure nickel coatings [14,23,24].

The electrodeposition process of composite coatings depends on many operating parameters. However, three main factors can be identified as influencing the composite electrodeposition process: particle type and concentration in electrolyte solution, the applied current density, and hydrodynamic condition [25]. Thus, the present work focuses mainly on the determination of the effect of these parameters on the electrodeposition process of Ni–W/ZrO_2 composites from sulphate–citrate plating bath containing zirconia nanopowder in suspension in order to find the optimum fabrication conditions. Microstructural and mechanical characteristics of the obtained Ni–W/ZrO_2 composites that were directly related to the electrodeposition conditions were also determined.

2. Experimental details

Ni–W/ZrO_2 composite coatings of a thickness about 5–30 μm were electrochemically deposited from aqueous plating solutions containing analytical grade pure chemicals: 0.1 M $NiSO_4$, 0.2 M Na_2WO_4, 0.5 M $Na_3C_6H_5O_7$, 0.3 M NH_4Cl, (5–30 g/L) ZrO_2 of pH 8 adjusted by an addition of sulphuric acid. The electrolysis was carried out in 0.75 dm^3 cell at temperature of 60 °C, under a galvanostatic regime (in the current density range of 5–11 A/dm^2), in a system with a rotating disk electrode (RDE) located in an external ultrasonic generator of variable frequency (35 kHz and 130 kHz) (Fig. 1).

The ferritic steel disks (0.028 dm^2) rotating at 340 rpm, supplied by potentiostat/galvanostat PAR 273A, were used as a cathode. Steel substrates were chemically polished in the solution of hydrogen peroxide and oxalic acid prior to electrolysis. The

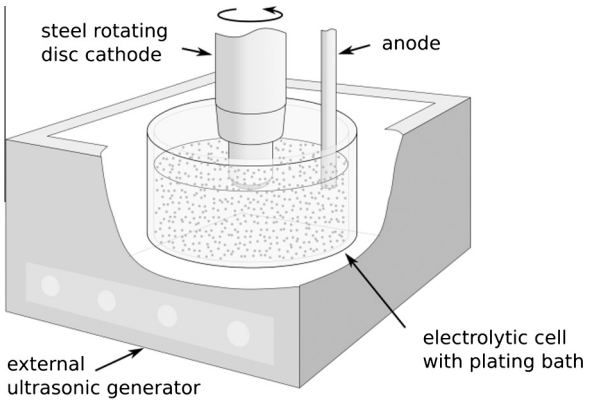

Fig. 1. The experimental setup with the rotating disc electrode (RDE) in an external ultrasonic field for composite coatings electrodeposition.

platinum spiral (~0.05 dm^2) was used as an anode. After electrolysis the samples were ultrasonically cleaned in ethanol for 1 min to remove loosely adsorbed particles from the coating surface, and then dried. The masses of deposits were determined by the analytical balance KERN ALT 220-5DAM. The coating thicknesses were estimated based on the deposit weight and the cross-section observations.

It is well known that the dispersion of ceramic nanoparticles in a plating bath is a very important stage of the electrodeposition process that strongly influences the nanocomposite properties [21,23]. To suppress or prevent agglomeration, prior to plating process the zirconia nanoparticles were mechanically dispersed in the bath using a stirrer (500 rpm) for 24 h. During the last 5 h, the suspension was additionally treated by ultrasounds. In part of the experiments, the polyelectrolyte PDADMAC [Poly (diallyldimethylammonium chloride)] was used as a dispersant. The zeta potential and the size distribution of zirconia particles in the plating bath (diluted hundred times) after mechanical stirring for 24 h before use were determined by a Zeta Sizer Nano ZS ZEN3500 analyser (based on the laser light-scattering technique). The X-ray diffraction technique (Bruker D8 Discover) was used to determine phase composition and an average grain size of deposits (Cu Kα filtered radiation). The crystallite size of the coatings was evaluated using Rietveld algorithms in MAUD software [26]. Structural characterization of the Ni–W/ZrO_2 coatings was complemented by SEM (FEI XL-30 E-SEM) and TEM (TECNAI) microstructural studies. Thin foils for TEM observations were prepared using focused ion beam (FIB) technique. Chemical composition of the coatings was determined by energy dispersive spectroscopy (EDS) analysis in SEM equipped with an EDAX Genesis 4000 spectrometer, on the cross section areas of the specimens, and a mean value was calculated from a minimum of six measurements. The values of microhardness and Young's modulus were measured during an indentation test with a Vickers diamond indenter according to ISO 14577-1 standard (Micro-Combo-Tester, CSEM Instrument). The adhesion of the coatings to the substrate has been measured by the micro-scratch technique using a Rockwell C spherical diamond stylus. The wear properties of coatings were evaluated using a ball-on-disc apparatus with alumina balls of 1 mm in diameter as the counter body. The investigations were conducted at established test parameters: wear track of 5 mm diameter, rotation speed of 60 rpm, normal load of 1 N and 20,000 a total number of cycles. The depth of wear track (~1 μm) was low compared to coating thickness. After tests, profiles of the wear tracks were measured with a stylus profilometer, that allowed to calculate the area of worn material. Wear rate W_V was calculated from the equation: $W_V = V/F_N \cdot S$, where: V – worn volume of material, F_N – applied load and S – sliding distance.

For comparison, metallic Ni–W coatings were also prepared using the bath of the same chemical composition but without the ZrO_2 suspension, under the same electrodeposition conditions.

3. Results and discussion

3.1. Zirconia particle characterization

ZrO_2, as an extremely refractory compound, is commonly used in composites as the second phase due to its high hardness (13 GPa), high density (6 g/cm^3), low thermal conductivity (11×10^{-6} K^{-1}), wear resistance and an excellent combination of high fracture toughness (~10 MPa m$^{1/2}$) and high flexural strength (~1 GPa) as well as high temperature oxidation resistance. However, these properties vary significantly depending on crystallographic structure. Zirconia is a polymorphic material with three crystallographic structures: monoclinic (*m*), tetragonal (*t*) and cubic (*c*). At very high temperatures (>2370 °C), only the cubic phase exists. At intermediate temperatures (1170–2370 °C), the tetragonal structure becomes thermodynamically stable. Below 1170 °C, the material transforms to the monoclinic structure [27]. Zirconia stabilized in the tetragonal structure exhibits the ability to stress-induced transformation toughened, avoiding cracking and mechanical weakening. The deformation energy of the material is absorbed by the phase transformation ($t \rightarrow m$), impeding the crack propagation. The transformation from the tetragonal to monoclinic phase occurs with a volume expansion (by a 3–5%) and a shear distortion parallel to the basal plane of *t*-ZrO_2. This mechanism leads to the high fracture toughness of tetragonal zirconia [28]. Some oxide additives, e.g., as the stabilizer Y^{3+} in Y_2O_3, can suppress $t \rightarrow m$ transformation of ZrO_2 and reduce the transformation temperature. Indeed, an addition of 3 mol% of Y_2O_3 enables the stabilization of the high-temperature tetragonal phase at room temperature. Thus, the tetragonal phase reveals (at ambient temperature) superior mechanical properties, such as fracture toughness and wear resistance. However, the toughened zirconia shows a degradation of properties with increasing temperature, and it is generally limited to use below 800 °C.

The commercial zirconium(IV) dioxide nanopowder 3 mol% Yttria stabilized (YTZP) (3Y-ZrO_2) produced by M/s Nanostructured and Amorphous Materials, Inc. (USA) (hereafter referred to as ZrO_2) was selected for the deposition of Ni–W alloy matrix composites. ZrO_2 powder has been previously characterized by the XRD and TEM techniques. Fig. 2 shows the X-ray diffraction pattern of ZrO_2 powder, whereas Fig. 3 presents the corresponding TEM image. Detailed XRD studies revealed that the ZrO_2 powder is not fully tetragonal but consists of a mixture of the tetragonal, monoclinic and cubic phases (of the smallest amount). Moreover, each phase is characterized by a different crystallite size in the range of 45–145 nm (Table 1). An average ZrO_2 grain diameter was estimated to about 50 nm based on the isotropic size-strain model of the Rietveld method analysis. The average particle size (confirmed by TEM examination) is compatible with that given by the manufacturer (50 nm).

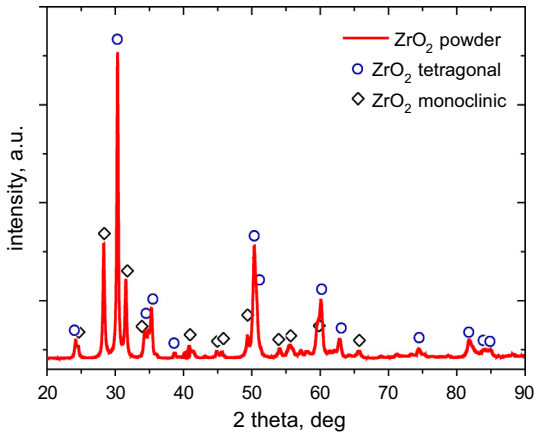

Fig. 2. X-ray diffraction pattern of the ZrO_2 nanopowder.

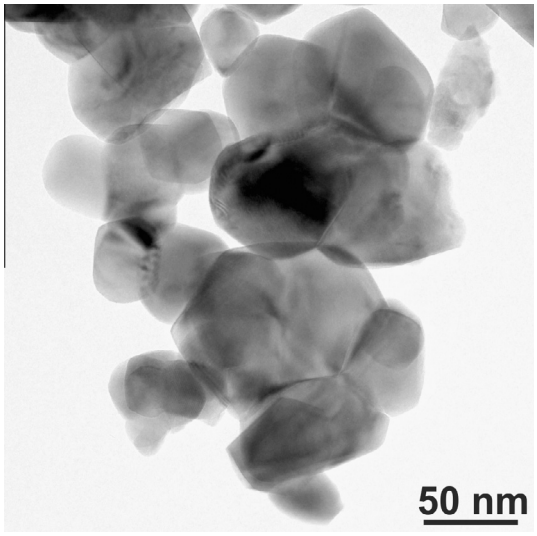

Fig. 3. TEM image of zirconia nanoparticles.

The TEM image (Fig. 3) shows the ZrO_2 nanoparticles to be almost spherical (equiaxed) with diameters in the range of 40–60 nm. As shown previously for the Ni–W/Al_2O_3 composite system, shape and phase compositions of nanoparticles are crucial parameters affecting the content and uniform distribution of ceramic particles much more than their size in the nanometer range (<100 nm). It was established that in contrast to the multiphase Al_2O_3 nanoparticles of irregular crystallites, the monophasic α-Al_2O_3 of spherical shape embedded much more easily and more uniformly in the nanocrystalline Ni–W alloy matrix, resulting in an increase of composite ceramic fraction (even 10 times) and a substantial increase in hardness [14].

3.2. Plating bath characterization

In the process of MMC electrochemical deposition, particle dispersed coatings are electroplated on a steel disk cathode substrate from an aqueous plating bath containing inert ceramic particles (in suspension) and ions of metals forming the matrix. Ceramic particles form with the electrolyte solution the heterogeneous, thermodynamically unstable binary system, the durability of which depends mainly on the type, dimension, shape and concentration of particles as well as on the nature and ionic strength of the basic electrolyte. Incorporation of the ceramic particles into a metallic

Table 1
XRD phase analyses and the estimation of the crystallite size in ZrO_2 powder.

Crystallographic phase	Monoclinic (m-ZrO_2)	Tetragonal (*t*-ZrO_2)	Cubic (*c*-ZrO_2)
Temperature range, °C	<1170	1170–2370	2370–2680
Space group	$P2_1/c$	$P4_2/nmc$	$Fm3m$
Mechanical properties	Poor	Superior	Good
Wt.% in 3Y-ZrO_2 powder	45.3 ± 2.0	40.6 ± 2.0	14.1 ± 2.5
Crystallite size of 3Y-ZrO_2, nm	44.9 ± 6.0	64.5 ± 17.5	145 ± 70

matrix requires the stable suspension of powder in an electrolyte solution, which is very difficult to obtain, especially for nanoparticles. Moreover, ultrafine particles exhibit a strong tendency to agglomerate in the galvanic bath due to high surface activity. Also, the usually high ionic strength of electroplating baths promotes the particle agglomeration, and even at higher ionic strength or low surface charge, the particles can agglomerate irreversibly [29,30].

Unique functional properties of MMC coatings depend not only on the amount of the particles, but more importantly on their size and uniform distribution in the bulk of the metallic matrix, which is related to particle characteristics, parameters of the basic electrolyte solution (chemical composition, additive type and concentration), and operating parameters of the electrolysis process. The agglomeration of particles in the matrix significantly degrades the mechanical properties of resulting composites, so obtaining a homogeneous distribution of the ceramic nanophase in coatings is a fundamental issue for MMC technology. It is well known that the distribution of nanoparticles in the deposits is closely correlated with dispersion of nanoparticles in the plating bath [16]. Hence, a crucial stage in MMC electrodeposition is the achievement of a stable, homogeneous dispersion of nanoparticles in solution. Various physical and chemical methods are used for particle de-agglomeration [25]. Different additives (anionic, cationic, nonionic), such as sodium dodecyl sulphate (SDS) and hydroxypropylcellulose (HPC), have been studied to reduce the particle agglomeration [31].

In the deposition process of the Ni–W/ZrO_2 composite, insoluble ZrO_2 ceramic particles suspended in the multicomponent bath are embedded in the Ni–W alloy matrix, which is simultaneously growing on the cathode. Due to ionic nature and a chemical interaction with the plating solution, the ZrO_2 powder undergoes surface modification, and particles dispersed in a solution are electrically charged. The surface charge affects the distribution of electrolyte solution ions in the interfacial area, resulting in an increased concentration of counter ions close to the particle surface. Thus, an electrical double layer is formed at the particle-solution interface. Obviously, an addition of a surfactant to the plating bath generally alters the surface charge of the particles. The zeta (electrokinetic) potential is the main measure of the surface charge of particles. The value of the zeta potential (surface charge) and the size distribution of ZrO_2 particles determined in a diluted bath containing W(VI) and Ni(II) citrate complex ions are presented in Table 2.

As shown in Table 2, the zeta potential of ZrO_2 particles in the electrolyte solution is highly negative (practically independent of particle concentration), due to specific adsorption of citrate anions. However, despite having a zeta potential of about −60 mV, the suspension was found to be unstable (±30 mV being considered a suitable threshold value for stability). The effective diameter of ZrO_2 particles in the plating bath was determined to be about 170 nm. To maintain the plating bath stability and to achieve a smaller size of ZrO_2 aggregates as well as a shift of the zeta potential towards positive values, the cationic polyelectrolyte PDADMAC (Poly (diallyldimethylammonium chloride)) was used as a dispersant.

Table 2
Zeta potential (mV) and particle size (nm) for different zirconia concentrations (g/L) in the plating bath.

ZrO_2 concentration (g/L)	Zeta potential (mV)	Particle size (nm)
20	−61.2	170
60	−62.2	170
80	−62.6	190
100	−64.5	170
120	−63.3	150

Polyelectrolytes can easily be adsorbed onto the surface of ZrO_2 nanoparticles, providing an organic barrier, which prevents particle agglomeration in suspension. It was also expected that the positive surface charge can improve the particle transport towards the negatively charged cathode by electrophoresis and facilitate the electrostatic adsorption of suspended particles on a cathode surface, enhancing the particle incorporation into the matrix [2]. Zeta potentials of zirconia particles in the plating solution with the PDADMAC addition were measured by dynamic light scattering (DLS) and shown in Fig. 4. As can be seen, with the increasing concentration of polyelectrolyte $(C_8H_{16}NCl)_n$, an increase of zeta potential up to +35 mV is observed, due to the adsorption of the cationic dispersant on the particle surface. The cationic polyelectrolyte in the plating bath slightly diminishes the agglomeration and helps to obtain homogeneous distribution of the particles. This distribution was about 140 nm, whereas it was almost 170 nm without surfactant. It was also found that introduction of PDADMAC into the solution improves the bath stability. The particles remained uniformly distributed without sedimentation during a few days mainly due to the mutual repulsion and increasing viscosity of the solution [32]. Similarly, it has been reported that polyelectrolyte dispersant containing aromatic rings (PEDA) to disperse zirconia nanoparticles in Ni–ZrO_2 plating bath has been successfully applied [21].

The effect of PDADMAC polyelectrolyte on the electrodeposition of composite coatings was studied at a particle concentration in electrolyte solution of 5 g/L, current density of 7 A/dm^2, under forced convection conditions corresponding to the rotation of a steel disk cathode at 340 rpm. The results obtained suggest that incorporation of ZrO_2 particles inhibits the deposition process of Ni–W alloy (forming a matrix of the composite) due to a reduction of the electroactive surface of the cathode and its polarization (Table 3). The effect is significantly intensified in the presence of the polyelectrolyte addition in the plating bath, which additionally adsorbs on the cathode. The cathodic current efficiency of Ni–W electrodeposition decreases about three times compared to the bath without the addition. From the results presented in Table 3, it is interesting to observe that the amount of embedded ZrO_2 particles in the coating slightly diminishes in presence of the addition of PDADMAC, despite the positive zeta potential. The lack of the beneficial effect of cationic surfactants on the amount of inert particles in electrodeposited composites that has been observed for different systems is contrary to other findings and assumptions for the promotion of particle co-deposition by surfactants [33]. This effect could indicate either a low impact of electrophoretic

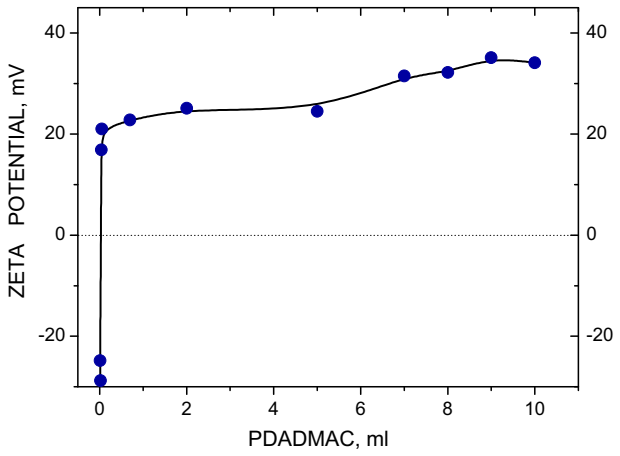

Fig. 4. Zeta potential of ZrO_2 particles in increasing concentration of the cationic polyelectrolyte $(C_8H_{16}NCl)_n$ (volume of 0.02% solution).

Table 3
Chemical composition (wt.%) of Ni–W and Ni–W/ZrO_2 coatings and current efficiency (%) of alloy matrix deposition.

SYSTEM	ADDITION	Ni (wt.%)	W (wt.%)	ZrO_2 (wt.%)	Eff_{Ni} (%)	Eff_W (%)	Eff_{alloy} (%)
Ni–W	–	52	48	–	10.7	9.3	20
Ni–W/ZrO_2	–	47	47.7	5.3	9.1	8.9	18
Ni–W/ZrO_2	PDADMAC	42.2	54.5	3.3	3.2	3.8	7

migration in the zirconia incorporation process or a too high concentration of surfactant used, since the excess may adsorb on the cathode surface, increasing the effective current density. As shown further (Fig. 11), an increase of the current density results in a decrease of the particle content in the composite coatings. Moreover, an excess of surfactant can be incorporated into deposits, which generally leads to brittle coatings.

Fig. 5 shows the backscattered SEM (BSE) images of the surface and a cross section of Ni–W/ZrO_2 composite coating obtained in presence of the polyelectrolyte in the plating bath. The zirconia particles appear black against the grey Ni–W matrix. The composite coatings were compact and well adhered to the steel substrate and characterized by a smoother surface compared to the coatings deposited from the bath without the addition. The ZrO_2 particles were found to be distributed more homogeneously in the matrix.

3.3. Effect of ultrasonication

Besides chemical treatment using a suitable surfactant, agglomeration of nanoparticles can be avoided to a significant extent by physical dispersion, including ultrasound (US). Ultrasound is often applied to prepare a stable suspension of ceramic particles in the electrolyte solution prior to the composite plating, whereas the use of US treatment during electrolysis is not common. However, some reports indicate a beneficial effect of US-assisted

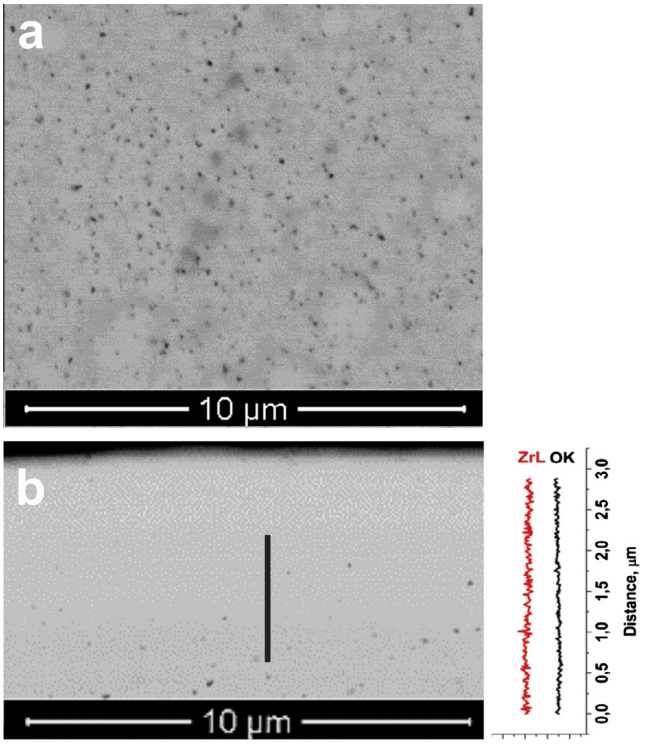

Fig. 5. SEM image (BSE) of the surface (a) and cross section image with EDX signal for Zr–L and O–K along the linescan (b) of Ni–W/ZrO_2 (42 wt.% Ni, 55 wt.% W, 3 wt.% ZrO_2) composite coating deposited from a plating bath containing 5 g/L ZrO_2 of pH 8 in the presence of PDADMAC addition (7 A/dm^2, 60 °C, 340 rpm).

electrodeposition of composites compared to the conventional silent procedure [34–36]. The propagation of US waves in the plating bath generates high pressure, causing stress that promotes the separation of individual nanoparticles from agglomerates [36]. Moreover, the cavitation effect can enhance the diffusion processes, remove the hydrogen bubbles adsorbed on the cathode, and clean and activate its surface. In most of the work presented in the literature, a US probe directly immersed into the plating bath was the source of ultrasonic energy [35,36]. Instead, in the present study, the cell containing the electrolyte solution was immersed in an external ultrasonic generator (heated US bath) with a frequency of 35 kHz and 130 kHz. Ni–W/ZrO_2 composite coatings were obtained in the ultrasonic field, as well as in silent electrodeposition. It was found that under ultrasonic treatment (at 35 kHz), the ZrO_2 particle incorporation into the Ni–W matrix increases significantly. For example, an enhancement of particle content from 1.7 wt.% to 4.7 wt.% in coatings deposited at 7 A/dm^2, from plating solution containing 10 g/L was observed. At the same time, the tungsten content in Ni–W alloy matrix decreases about 3 wt.%. Ultrasonication also results in a slight increase in cathodic current efficiency (about 5%), due to a decrease of hydrogen incorporation in the coatings. The enrichment of zirconia nanoparticle embedding observed under ultrasonication is mainly related to two synergic effects, i.e., the acceleration of the particle transport to the cathode surface and de-agglomeration (breaking up and preventing the agglomerate formation) [34–36]. It is known that separate individual nanoparticles exhibit greater opportunity than the agglomerated particle groups to be co-deposited due to stronger attraction by the electric field, making effective strong adsorption on the cathode surface [29]. In contrast, the decrease of the ZrO_2 content incorporated in the coatings deposited under the higher US frequency studied (130 kHz) has been observed. The effect could be compared to excessive bath agitation, which causes the loosely adsorbed nanoparticles to be removed from the cathode surface before they are co-deposited [14,24,37,38]. Thus, in further experiments the frequency of 35 kHz was accepted as the most favourable for sufficient nanoparticle incorporation. A similar US frequency for the deposition of Ni–Co/Al_2O_3 alloy matrix composite has also been chosen [38].

The pure Ni–W metallic coatings electrodeposited under silent electrodeposition exhibit a regular pyramidal-like surface morphology (Fig. 6a). The introduction of zirconia particles into the electrolyte solution changes the surface morphology. Indeed, the composite coatings fabricated without US show incoherent, globular surface morphology (Fig. 6c). At higher current density (11 A/dm^2), the coating surface becomes more developed and larger cauliflower-like structures were formed (Fig. 6e). Ultrasonication results in a substantial surface modification. The surface morphologies of all coatings obtained were changed to more regular, smooth, compact and homogeneous with a reduction of roughness (Fig. 6b, d and f). Moreover, the composite coatings obtained with ultrasonication treatment show a uniform chemical composition across the thickness. The application of US enhances homogeneous, well-dispersed particle incorporation. TEM observations confirmed that the presence of ultrasound considerably reduces the particle agglomeration and promotes a uniform dispersion of ZrO_2 nanoparticles in the Ni–W matrix (Fig. 7a). The Ni–W matrix was characterized, nanocrystalline grains of an average size below 10 nm. HRTEM image shows good interconnection between phases (ceramic particles and the metallic matrix), the lack of voids and discontinuity at the interface (Fig. 7b).

3.4. Effect of ceramic particle concentration

For a wide range of MMC systems, the inert particle composite content increases to a certain limiting value reached at higher

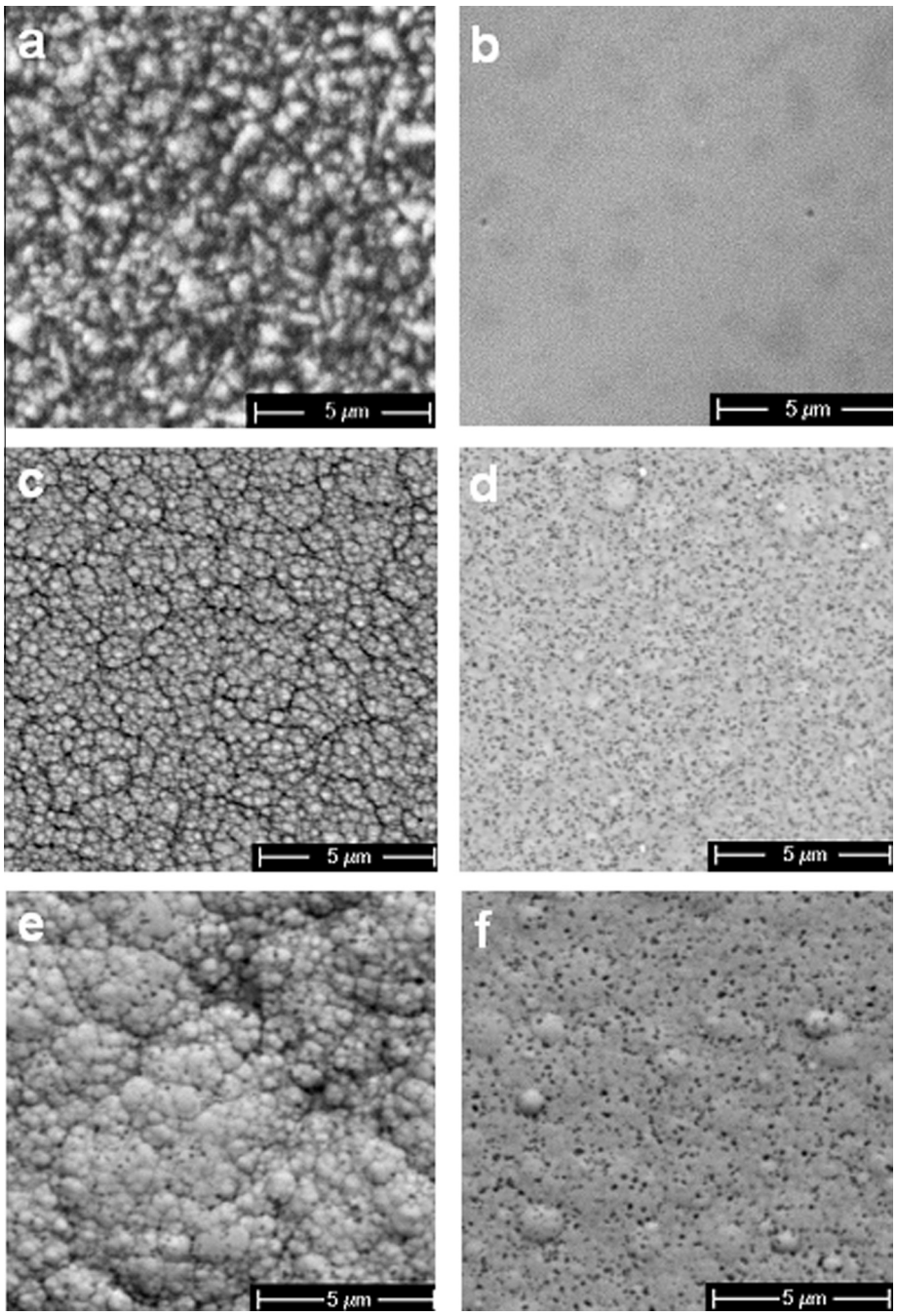

Fig. 6. SEM surface images of coatings electrodeposited under the silent condition (a, c, e) and sonication (b, d, f) as follows: metallic Ni–W (a, b), composite Ni–W/ZrO_2 deposited at 7 A/dm^2 from solution containing zirconia powder of 10 g/L (c, d) and deposited at 11 A/dm^2 from solution of 5 g/L ZrO_2 nanoparticles (e, f).

particle bath concentration [33]. The behaviour is related to the particle adsorption at the cathode surface according to a Langmuir adsorption isotherm, and corresponds to the first stage (i.e., the physical loose adsorption) in a successive two-step adsorption mechanism for incorporation of inert particles during electrodeposition proposed by Guglielmi [39]. Such dependence was observed for a Ni–W/ZrO_2 composite deposited from a citrate bath containing zirconia in the concentration range of 2.5–5 g/L, in the presence of sodium dodecyl sulphonate [40]. In contrast, in the present study, for incorporation of zirconia particles in the Ni–W matrix, a deviation from the Langmuir adsorption behaviour at higher particle concentration in the electrolyte bath was observed. The weight percentage of the ZrO_2 particles in the composites increases continuously by raising concentration of zirconia powder in the plating solution (Fig. 8). At the same time, the tungsten content in Ni–W/ZrO_2 coatings decreases gradually from 50 wt.% to 43 wt.% with the increase of zirconia concentration from 5 g/L to 30 g/L in the plating bath. A similar effect was observed for electrodeposited Ni–W/Al_2O_3 and Ni–W/diamond composite coatings [14,41]. An increase of ZrO_2 composite content at a high particle bath concentration may be caused by the impact of hydrodynamics (RDE under ultrasonicated conditions) or additional particle adsorption at sites that were not accessible at low particle concentration [33]. Also, a higher concentration of particles in the plating bath can enhance the adsorption rate on the cathode surface, thus resulting in a higher content of co-deposited ZrO_2 nanoparticles

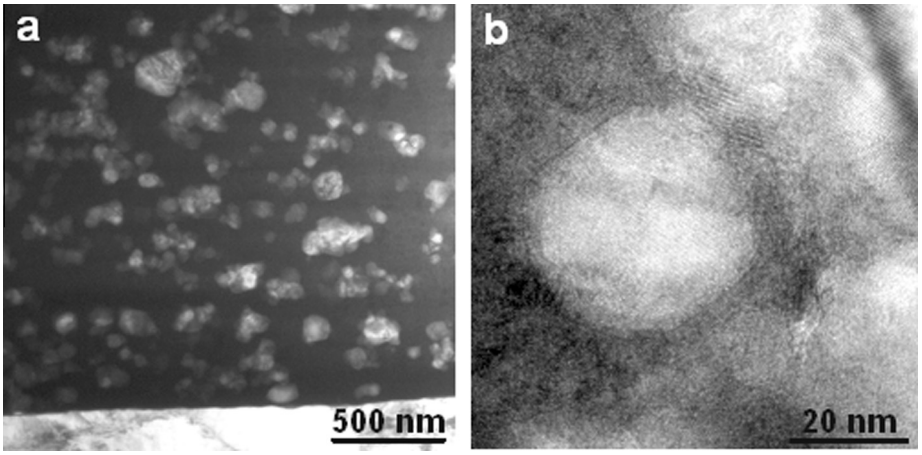

Fig. 7. TEM (a) and HRTEM (b) images of a cross section of Ni–W/ZrO_2 coating electrodeposited with ultrasonication (35 kHz) from the plating bath containing 20 g/L zirconia particles (7 A/dm^2, 340 rpm).

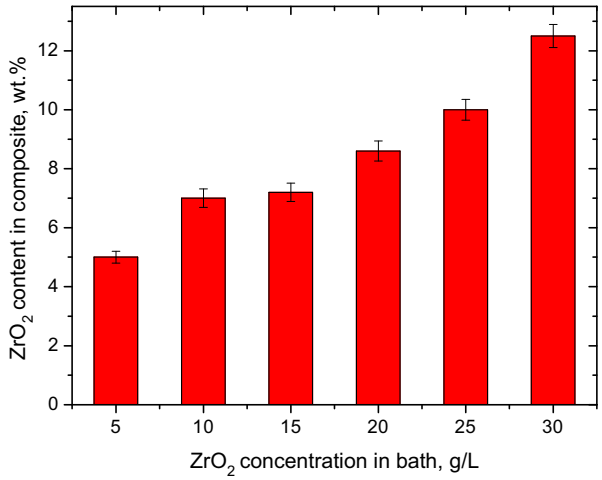

Fig. 8. Effect of ZrO_2 concentration in the plating bath on wt.% incorporation of ZrO_2 in the Ni–W/ZrO_2 composite coatings deposited in ultrasonic field of 35 kHz, at 7 A/dm^2, 60 °C, in a hydrodynamic condition corresponding to the cathode rotation speed of 340 rpm.

[16]. A decrease in particle composite content at higher particle bath concentration, due to settling and agglomeration of the particles is also reported in the literature [33].

Regardless of the amount of embedded ceramic phase, the Ni–W/ZrO_2 composite coatings obtained are of high quality, homogenous, smooth and compact and adhere well to steel substrates. Fig. 9 shows the SEM images of the surface and cross section of the Ni–W/ZrO_2 composite coatings electrodeposited from the nickel-tungsten plating bath containing 5 g/L and 30 g/L zirconia particles. As seen, ZrO_2 particles are uniformly distributed throughout the Ni–W matrix (from the steel substrate to surface of the coatings), even for the highest examined concentration of ZrO_2 in the bath. Lack of visible aggregates of zirconia particles was observed. Fig. 10 presents XRD patterns of Ni–W/ZrO_2 coatings deposited at different ZrO_2 particle loadings of the electrolyte solution. All the as-deposited coatings are characterized by a similar pattern showing only Ni and ZrO_2 diffraction peaks (the Fe peaks originated from the steel substrate).

The most intensive peak, located at $2\theta = 44°$, corresponds to the Ni (1 1 1) reflection. The relative intensity of ZrO_2 fits well to the particle content in deposits. XRD analysis reveals also that the electrodeposited Ni–W matrix is composed of a nanocrystalline face-centred cubic single phase (supersaturated solid solution of tungsten in nickel) and embedded zirconia consists of tetragonal and monoclinic phases. With increasing ZrO_2 particle content, the lines of Ni on XRD patterns increasingly broadened and their intensities slightly decreased as the microstructure of Ni–W matrix becomes more fine grained. Similarly, ZrO_2 nanoparticles perturb the growth of the nickel matrix of Ni/ZrO_2 composites, resulting in the formation of finer grains [21]. The mean crystallite size (the size of the coherent domains) of the Ni–W matrix, estimated using model in Rietveld algorithm (MAUD software [26]), is in the range below 10 nm, whereas the average zirconia particle sizes are 45 nm and 50 nm for tetragonal and monoclinic phases, respectively. It should be noted that the average particle size is also confirmed by TEM examination.

3.5. Effect of current density

In addition to the particle concentration, the current density is the most widely investigated parameter in MMC electrodeposition, wherein the direct current (DC) has most commonly been used. Current density is a very important operating variable in electrochemical technology, since it controls the electrodeposition rate, current efficiency, the chemical composition and microstructure, strongly affecting the functional properties of the resulting coatings. For MMCs, two main types of current density dependencies can be distinguished [33]. The inert particle composite content with current density either decreases or increases continuously or exhibits maxima, which is mostly related to the metals deposition behaviour [3,42]. However, some authors found little or no influence of current density on the particle incorporation [2].

In the present study, keeping the concentration of the particles (5 g/L), bath temperature (60 °C) and disk cathode rotation speed (340 rpm) constant, the current density was investigated in the range of 5–11 A/dm^2. Fig. 11 shows the influence of the current density on the ZrO_2 content in Ni–W/ZrO_2 coatings. As can be seen, the weight percentage of the co-deposited ZrO_2 nanoparticles decreased with an increase in current density (in the tested range). Similar results were reported for other systems, e.g., Cu–ZrO_2 composites [43]. At higher current densities, an enhanced deposition of metals occurs and particle incorporation becomes mainly diffusion controlled due to less accessibility of ZrO_2 particles with respect to the higher deposition rate of Ni–W alloys [44]. Thus, a continuously decreasing particle composite content with increasing current density was observed. It should be also noted that the current efficiency of the coating deposition increases over a range

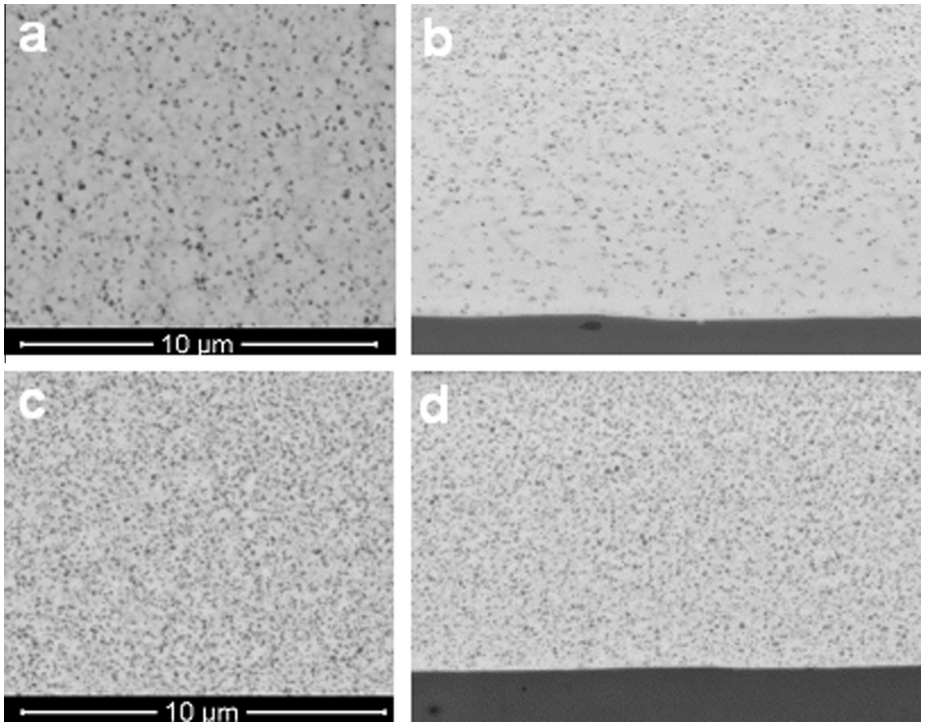

Fig. 9. SEM (BSE) image of the surface (a, c) and cross section (b, d) of Ni–W/ZrO_2 composite coatings electrodeposited from the plating bath with ZrO_2 particle loading of 5 g/L and 30 g/L, respectively (35 kHz, 340 rpm).

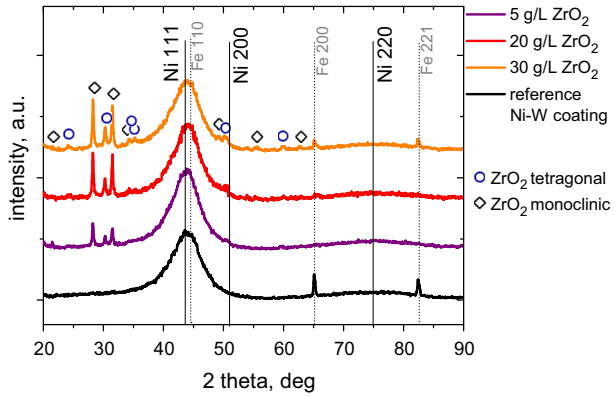

Fig. 10. XRD patterns (Cu Kα line) of metallic Ni–W and composite Ni–W/ZrO_2 coatings deposited from the electrolyte baths loaded with different amounts of ZrO_2, at 7 A/dm^2 (35 kHz, 340 rpm).

of tested current densities from 18% to 37%, at 5 A/dm^2 and 11 A/dm^2, respectively. Current efficiency is a part of electrical charges consumed for the deposition of nickel and tungsten, forming the Ni–W alloy. The remaining difference of the total charge is utilized for hydrogen evolution (cathodic side reaction). The change in the plating rate as a function of current density is also shown in Fig. 11. The plating rate refers to the final thickness of the composite coatings electroplated during 1 h. Fig. 12 shows, for example, SEM surface images of Ni–W/ZrO_2 coatings obtained at two different current densities (5 A/dm^2 and 8 A/dm^2). Homogeneous distribution of zirconia particles within the metallic matrix in the whole studied DC range was observed (Fig. 12a and c). However, when higher current densities were applied (>7 A/dm^2), the surface morphology changed from dense and compact to rough and globular, wherein the globule size increases with a further rise of current density (Fig. 12b and d).

It is known that finer-grained deposits are the result of conditions that favour crystal nuclei formation, such as increasing current density. Generally, decreasing crystallite size is the result of factors that increase the cathode polarization [45]. Thus, with increasing cathodic current density values, a composite coating with a smaller grain size matrix should be obtained.

However, practically no impact of the current density on the further microstructure refinement of Ni–W alloy matrix was observed. For the range tested (5–11 A/dm^2), current density variation does not affect the peak width of XRD spectra recorded for composites, as shown in Fig. 13. An increase of DC density value does not bring about the expected decrease in grain size, while the dispersion phase addition reduces it slightly (Fig. 10).

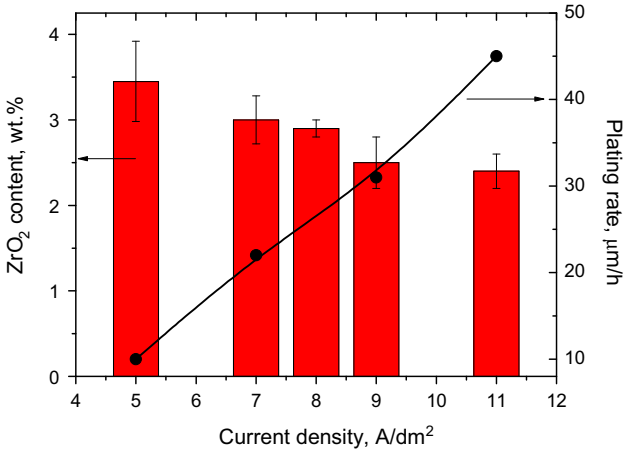

Fig. 11. Effect of the current density on the plating rate (µm/h) and the ZrO_2 content (wt.%) in Ni–W/ZrO_2 coatings obtained with 5 g/L particle loading in plating bath (35 kHz, 340 rpm).

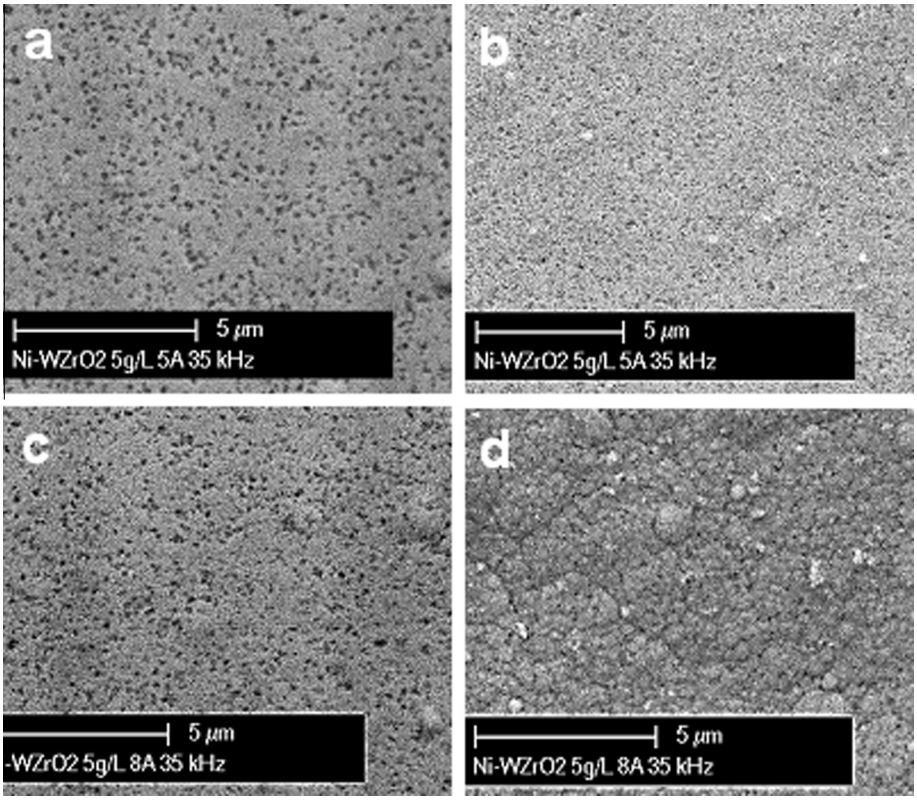

Fig. 12. SEM surface images (BSE and SE) of Ni–W/ZrO_2 composite coatings deposited at 5 A/dm^2 (a, b) and 8 A/dm^2 (c, d) obtained with 5 g/L particle loading in plating bath.

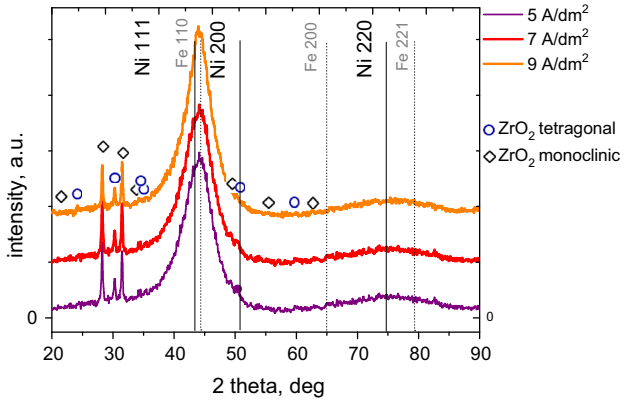

Fig. 13. XRD patterns (Cu Kα) of Ni–W/ZrO_2 composites deposited at different current densities.

3.6. Mechanical properties

The hardness of composite coatings is mainly determined by the microstructure of the matrix and properties of reinforced particles in the coatings. The microhardness value and Young's modulus of the Ni–W/ZrO_2 composites were measured during an indentation test with a Vickers diamond indenter according to ISO 14577-1 standard. Microindentation tests revealed that all as-deposited composite coatings obtained are characterized by a very good microhardness, which varied from about 8.5 GPa to 9.0 GPa, and a Young's modulus value from 190 to 200 GPa, depending on ZrO_2 particle content (Table 4). Moreover, the microhardness of the composite coatings is about 1 GPa higher than metallic Ni–W coatings. Thus, the ZrO_2 nanoparticles co-deposited in the Ni–W alloy matrix can restrain the plastic deformation of the matrix under loading, mainly due to enhanced dispersion strengthening effects. However, as shown in Fig. 14, the coating microhardness slightly decreases with increasing zirconia concentration in the electrolyte solution (over the tested range of 5–30 g/L). A similar effect was also observed for Ni/ZrO_2 composites deposited from a Watts type bath containing 10 g/L zirconia particles of 30 nm [20]. Other authors have observed for the Ni–W/ZrO_2 composites that microhardness of composites increasing with the increase in weight percentage of ZrO_2 nanoparticles in the coatings, deposited from a bath of 2.5–5 g/L zirconia concentration (Table 5) [19]. In practice, the most important parameter determining the mechanical properties of materials is the plasticity

Table 4
Chemical composition and micromechanical properties of Ni–W and Ni–W/ZrO_2 coatings of varying zirconia content (average thickness about 15 μm): H_{IT} – microhardness, E – elastic modulus, H_{IT}/E – plasticity index, h_{max} – maximum penetration depth, W_v – wear index.

ZrO_2 (wt.%)	W (wt.%)	H_{IT} (GPa)	E (GPa)	h_{max} (nm)	H_{IT}/E	$W_v \cdot 10^{-6}$ (mm^3/Nm)
–	49.6 ± 1.0	7.6 ± 0.40	189 ± 8	525 ± 11	0.040	5.3 ± 0.8
5.0 ± 0.2	50.1 ± 1.0	9.1 ± 0.74	191 ± 20	491 ± 19	0.048	3.8 ± 0.5
7.6 ± 0.3	47.2 ± 0.9	8.9 ± 0.52	201 ± 18	488 ± 14	0.044	7.4 ± 1.5
8.6 ± 0.3	45.3 ± 0.9	8.2 ± 0.60	192 ± 10	509 ± 19	0.043	7.8 ± 2.1
12.5 ± 0.5	43.2 ± 0.9	8.3 ± 0.40	190 ± 12	511 ± 13	0.044	8.1 ± 2.2

index (H_{IT}/E). The Ni–W/ZrO_2 composite coating with the lowest particle content (about 5 wt.%) are characterized by the highest plasticity index and thus the best mechanical properties.

It is known that for metallic nanomaterials, at the smallest grain size range, the hardness does not increase with a further reduction in grain size, and the so-called inverse Hall–Petch behaviour is observed [20]. The ceramic particles in the metal matrix could prevent or suppress grain boundary migration and act as obstacles to dislocation movement and grain boundary sliding, increasing the hardness over the limit for the nanocrystalline metals [20]. However, these effects depend primarily on the amount of the particles, their size and distribution in the metallic matrix and metal-ceramic interface bonding.

It can be assumed that the zirconia particle–strengthened Ni–W coatings exhibit an improvement of hardness (compared to metallic coatings) due to grain stabilization and dispersion hardening of the metal matrix grains. XRD peak broadening of Ni–W/ZrO_2 composites show that the size of the metal matrix grains was not very much affected by the co-deposition of an increasing amount of ceramic particles. Nevertheless, it should be noted that with increasing the ZrO_2 content in composite coatings, a gradual diminution of tungsten in Ni–W alloy matrix is observed. Indeed, the tungsten content decreases progressively from 50 wt.% to 43 wt.% with the increase of zirconia concentration in the plating bath from 5 g/L to 30 g/L (Table 4). This effect may be responsible for a slight hardness reduction in the resulting composite coatings. The mechanical properties of composites can also deteriorate due to a greater hydrogen evolution in the electrodeposition process (also in the deposits), accompanying the increasing zirconia powder concentration in the bath (polarization effect) [14,19,47]. In order to avoid the hydrogen defects and their influence on the composite mechanical properties, an adequate heat treatment is necessary. As can be seen from the data in Table 4, only the composite coating containing the smallest ZrO_2 content (5 wt.%) is characterized by a much higher wear resistance (wear index 3.8×10^{-6} mm^3/Nm) than Ni–W metallic coating (wear index 5.3×10^{-6} mm^3/Nm). However, further increase in the ZrO_2 content results in decrease in wear resistance of composite coatings. The effect is mainly due to the significant brittleness of coatings containing more than 5 wt.% ZrO_2, which is confirmed by the images of scratch tracks (Fig. 15). As is clearly visible, the nature of the deformation changes from plastic deformation to brittle fracture for composite enriched with zirconia. Moreover, cracking process is intensified with a further increase in the ZrO_2 content as shown by microscratch tests (Rockwell C using a spherical diamond stylus).

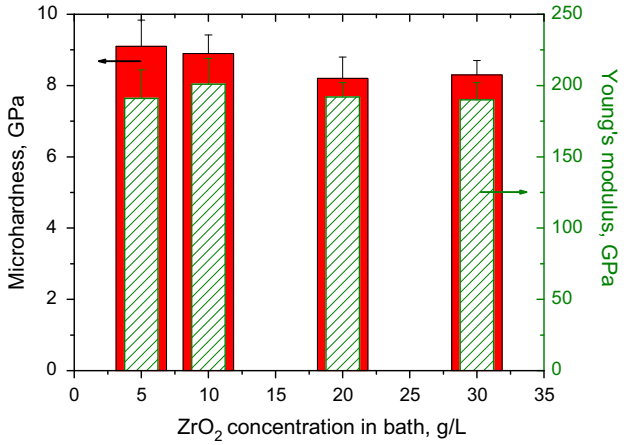

Fig. 14. Vickers microhardness and Young's modulus of Ni–W/ZrO_2 nanocomposite coatings deposited from the electrolyte solution with varying particle concentration.

4. Conclusions

The electrodeposition conditions for Ni–W/ZrO_2 nanocomposites have been developed. The Ni–W/ZrO_2 coatings with homogeneously dispersed zirconia particles can be produced by ultrasonication-assisted electrochemical co-deposition from an aqueous non-toxic (sulphate–citrate) electrolyte solution. Application of ultrasound promotes uniform particle distribution in the volume of the composite; however, the best results were obtained for the lower frequency. All composite coatings obtained (regardless of the current density and zirconia concentration in the bath) that were of grey-shiny appearance were crack free, homogenous, compact and well adherent to the steel substrate. The Ni–W

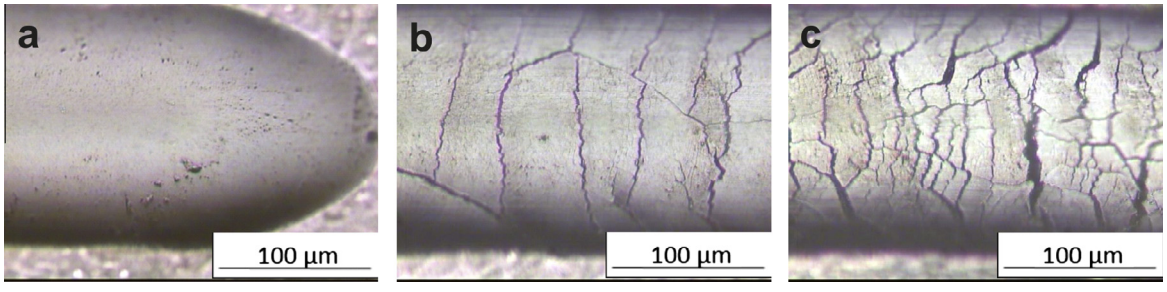

Fig. 15. LM images of scratch track of Ni–W/ZrO_2 coatings containing 5 wt.% (a), 7.8 wt.% (b) and 12.5 wt.% (c) of ZrO_2, respectively (load 30 N).

Table 5
Microhardness of Ni/ZrO_2 and Ni–W/ZrO_2 nanocomposite coatings obtained under different conditions.

Composite system	Size of ZrO_2 crystallites (nm)	Concentration range (g/L)	Phase composition	Vickers microhardness, HV	References
Ni/ZrO_2	4–10	10–50	Mixture of the tetragonal and monoclinic	300–500	[46]
Ni/ZrO_2	10–30	10	Not available	350–450	[20]
Ni–W/ZrO_2	50	2.5–5	Not available	500–700	[19]
Ni–W/ZrO_2	50	5–30	Mixture of the tetragonal and monoclinic	800–850	Present work

matrix consists of a nanocrystalline face-centred cubic single phase (supersaturated solid solution of tungsten in nickel) and is characterized by nanocrystalline grains of an average size below 10 nm. Good interconnection between phases (ceramic particles and the metallic matrix), the lack of voids and discontinuity at the interface was observed. These composite coatings exhibit a considerable enhancement in microhardness in comparison to pure Ni–W and composite Ni/ZrO_2 coatings. The Ni–W/ZrO_2 composites with the lowest particle content (about 5 wt.%) are characterized by the best mechanical properties.

Acknowledgement

The results presented in this paper were supported by the National Science Centre in the frame of the Project No. 2011/01/B/ST8/03974, entitled "Nanocomposite Ni–W/ZrO_2 coatings obtained by electrochemical deposition as an alternative to toxic chromium coatings – preparation, characterization and properties"

References

[1] U.K. Kainer, Metal Matrix Composites, Custom-made Materials for Automotive and Aerospace Engineering, WILEY-VCH Verlag GmbH & Co. KGaA, Weinheim, 2006.
[2] C. Kerr, D. Barker, F. Walsh, J. Archer, The electrodeposition of composite coatings based on metal matrix-induced particle deposits, Trans. Inst. Met. Finish. 78 (2000) 171–178.
[3] M. Yousefpour, A. Rahimi, Characterization and selection of optimal parameters to achieve the best tribological performance of the electrodeposited Cr nanocomposite coatings, Mater. Design. 54 (2014) 382–389.
[4] I. Brooks, P. Lin, G. Palumbo, G.D. Hibbard, U. Erb, Analysis of hardness-tensile strength relationships for electroformed nanocrystalline materials, Mater. Sci. Eng., A 491 (2008) 412–419.
[5] V. Viswanathan, T. Laha, K. Balani, A. Agarwal, S. Seal, Challenges and advances in nanocomposite processing techniques, Mater. Sci. Eng., R 54 (2006) 121–285.
[6] I. Gurrappa, L. Binder, Electrodeposition of nanostructured coatings and their characterization – a review, Sci. Technol. Adv. Mater. 9 (2008) 1–11.
[7] N. Kanani, Electroplating-Basic Principles. Processes and Practice, Elsevier, Amsterdam, 2006.
[8] S.T. Aruna, V.K. Grips, K.S. Rajam, Ni-based electrodeposited composite coating exhibiting improved microhardness, corrosion and wear resistance properties, J. Alloys Compd. 468 (2009) 546–552.
[9] D.E. Burns, Y. Zhang, M. Teutsch, K. Bade, J. Aktaa, K.J. Hemker, Development of Ni-based superalloys for microelectromechanical systems, Scripta Mater. 67 (2012) 459–462.
[10] T. Chookajorn, H.A. Murdoch, A. Schuh, Design of stable nanocrystalline alloys, Science 337 (2012) 951–954.
[11] A. Genc, M.L. Ovecoglu, M. Baydogan, S. Turan, Fabrication and characterization of Ni–W solid solution alloys via mechanical alloying and pressureless sintering, Mater. Design 42 (2012) 495–504.
[12] Z. Galikova, M. Chovancova, V. Danielik, Properties of Ni–W alloy coatings on steel substrate, Chem. Pap. 60 (2006) 353–359.
[13] P. Indyka, E. Beltowska-Lehman, L. Tarkowski, A. Bigos, E. García-Lecina, Structure characterization of nanocrystalline Ni–W alloys obtained by electrodeposition, J. Alloys Compd. 590 (2014) 75–79.
[14] E. Beltowska-Lehman, P. Indyka, A. Bigos, M. Kot, L. Tarkowski, Electrodeposition of nanocrystalline Ni–W coatings strengthened by ultrafine alumina particles, Surf. Coat. Technol. 211 (2012) 62–65.
[15] S. Yari, C. Dehghanian, Deposition and characterization of nanocrystalline and amorphous Ni–W coatings with embedded alumina nanoparticles, Ceram. Int. 39 (2013) 7759–7766.
[16] Y. Yao, S. Yao, L. Zhang, H. Wang, Electrodeposition and mechanical and corrosion resistance properties of Ni–W/SiC nanocomposite coatings, Mater. Lett. 61 (2007) 67–70.
[17] Y. Boonyongmaneerat, K. Saengkiettiyut, S. Saenapitak, S. Sangsuk, Effects of WC addition on structure and hardness of electrodeposited Ni–W, Surf. Coat. Technol. 203 (2009) 3590–3594.
[18] K. Arunsunai Kumar, G. Paruthimal Kalaignan, V.S. Muralidharan, Direct and pulse current electrodeposition of Ni–W–TiO_2 nanocomposite coatings, Ceram. Int. 39 (2013) 2827–2834.
[19] C. Zhao, Y. Yao, L. He, Electrodeposition and characterization of Ni–W/ZrO_2 nanocomposite coatings, Bull. Mater. Sci. 37 (2014) 1053–1058.
[20] W. Wang, F.Y. Hou, H.I. Wang, H.T. Guo, Fabrication and characterization of Ni/ZrO_2 composite nano-coatings by pulse electrodeposition, Scripta Mater. 53 (2005) 613–618.
[21] G.N.K. Ramesh Bapu, S. Jayakrishnan, Oxidation characteristics of electrodeposited nickel–zirconia composites at high temperature, Mater. Chem. Phys. 96 (2006) 321–325.
[22] K.F. Zhang, S. Ding, G.F. Wang, Different superplastic deformation behaviour of nanocrystalline Ni and ZrO_2/Ni nanocomposite, Mater. Lett. 62 (2006) 719–722.
[23] E. Beltowska-Lehman, A. Goral, P. Indyka, Electrodeposition and characterization of Ni/Al_2O_3 nanocomposite coatings, Arch. Metall. Mater. 56 (2011) 919–931.
[24] P. Indyka, E. Beltowska-Lehman, A. Bigos, Microstructural characterisation of electrodeposited coatings of metal matrix composite with alumina nanoparticles, Inst. Phys. Conf. Ser. – Mater. Sci. Eng. 32 (2012) 012010.
[25] C.T.J. Low, R.G.A. Wills, F.C. Walsh, Electrodeposition of composite coatings containing nanoparticles in a metal deposit, Surf. Coat. Technol. 201 (2006) 371–383.
[26] L. Lutterotti, P. Scardi, Simultaneous structure and size-strain refinement by the Rietveld method, J. Appl. Cryst. 23 (1990) 246–252.
[27] J. Chevalier, L. Gremillard, The tetragonal-monoclinic transformation in zirconia, J. Am. Ceram. Soc. 92 (2009) 1901–1920.
[28] M.C. Munoz, S. Gallego, J.I. Beltran, J. Cerda, Adhesion at metal-ZrO_2 interfaces, Surf. Sci. Rep. 61 (2006) 303–344.
[29] S.-L. Kuo, Y-Ch Chen, M.-D. Ger, W.-H. Hwu, Nano-particles dispersion effect on Ni/Al_2O_3 composite coatings, Mater. Chem. Phys. 86 (2004) 5–10.
[30] A. Gomes, I. Pereira, B. Fernandez, R. Pereiro, Electrodeposition of metal matrix nanocomposites: improvement of the chemical characterization techniques, in: Advanced in Nanocomposites – Synthesis, Characterization and Industrial Applications, Publisher InTech, 2011.
[31] M.-D. Ge, Electrochemical deposition of nickel/SiC composites in the presence of surfactants, Mat. Chem. Phys. 87 (2004) 67–74.
[32] R.J. Hunter, Zeta Potential in Colloid Science: Principles and Applications, Academic Press, UK, 1988.
[33] A. Hovestad, L.J.J. Janssen, Electroplating of Metal Matrix Composites by Codeposition of Suspended Particles, Modern Aspects of Electrochemistry, Academic/Plenum Publishers, New York, 2005.
[34] F. Su, C. Liu, P. Huang, Ultrasound-assisted pulse electrodeposition and characterization of Co–W/MWCNTs nanocomposite coatings, Appl. Surf. Sci. 309 (2014) 200–208.
[35] E. Garcia-Lecina, I. Garcia-Urrutia, J.A. Diez, J. Morgiel, P. Indyka, A comparative study of the effect of mechanical and ultrasound agitation on the properties of electrodeposited Ni/Al_2O_3 nanocomposite coatings, Surf. Coat. Technol. 206 (2012) 2998–3005.
[36] H.-Y. Zheng, M.-Z. An, Electrodeposition of Zn–Ni–Al_2O_3 nanocomposite coatings under ultrasound conditions, J. Alloys Compd. 459 (2008) 548–552.
[37] A. Bigos, E. Beltowska-Lehman, P. Indyka, J. Morgiel, Electrodeposition of nanocrystalline matrix Ni–Mo/Al_2O_3 composites, Composites 2 (2011) 157–162.
[38] D. Dietrich, I. Scharf, D. Nickel, L. Shi, T. Grund, T. Lampke, Utrasound technique as a tool for high-rate incorporation of Al_2O_3 in NiCo layers, J. Solid State Electrochem. 15 (2011) 1041–1048.
[39] N. Guglielmi, Kinetics of the deposition of inert particles from electrolytic baths, J. Electrochem. Soc. 119 (1972) 1009–1012.
[40] Ch. Zhao, Y. Yao, L. He, Electrodeposition and characterization of Ni–W/ZrO_2 nanocomposite coatings, Bull. Mater. Sci. 37 (2014) 1053–1058.
[41] K.-H. Hou, H.-T. Wang, H.-H. Sheu, M.-D. Ger, Preparation and wear resistance of electrodeposited Ni–W/diamond composite coatings, Appl. Surf. Sci. 308 (2014) 372–379.
[42] B.J. Hwang, Ch.S. Hwang, Mechanism of codeposition of silicone carbide with electrolytic cobalt, J. Electrochem. Soc. 140 (1993) 979–984.
[43] Y.Z. Wan, Y.L. Wang, H.M. Tao, G.X. Cheng, X.H. Dong, Preparation and characterization of different particles-copper electrocomposites, J. Mater. Sci. Lett. 17 (1998) 1251–1253.
[44] A.K. Chaudhari, V.B. Singh, Structure and properties of electro co-deposited Ni–Fe/ZrO_2 nanocomposites from ethylene glycol bath, Int. J. Electrochem. Sci. 9 (2014) 7021–7037.
[45] J.W. Dini, Electrodeposition: The Materials Science of Coatings and Substrates, Noyes Publications, USA, Westwood, New Jersey, 1993.
[46] A. Moller, H. Hahn, Synthesis and characterization of nanocrystalline Ni/ZrO_2 composite coatings, Nanostruct. Mater. 12 (1999) 259–262.
[47] H. Ferkel, B. Muller, W. Riehemann, Electrodeposition of particle-strengthened nickel films, Mater. Sci. Eng. A234–236 (1997) 474–476.